Chronic recording of hand prosthesis control signals via a regenerative peripheral nerve interface in a rhesus macaque



2016 J. Neural Eng. 13 046007

(http://iopscience.iop.org/1741-2552/13/4/046007)

IOP Publishing Journal of Neural Engineering
J. Neural Eng. 13 (2016) 046007 (11pp) doi:10.1088/1741-2560/13/4/046007

# Chronic recording of hand prosthesis control signals via a regenerative peripheral nerve interface in a rhesus macaque

**Z T Irwin[1], K E Schroeder[1], P P Vu[1], D M Tat[1], A J Bullard[1], S L Woo[2], I C Sando[2], M G Urbanchek[2], P S Cederna[1,2] and C A Chestek[1,3,4,5,6]**

[1] Department of Biomedical Engineering, University of Michigan, Ann Arbor, MI, USA
[2] Department of Surgery, Plastic Surgery section, University of Michigan, Ann Arbor, MI, USA
[3] Department of Electrical Engineering and Computer Science, University of Michigan, Ann Arbor, MI, USA
[4] Neuroscience Graduate Program, University of Michigan, Ann Arbor, MI, USA
[5] Robotics Graduate Program, University of Michigan, Ann Arbor, MI, USA

E-mail: cchestek@umich.edu

Received 10 February 2016, revised 26 April 2016
Accepted for publication 12 May 2016
Published 1 June 2016

**Abstract**

*Objective*. Loss of even part of the upper limb is a devastating injury. In order to fully restore natural function when lacking sufficient residual musculature, it is necessary to record directly from peripheral nerves. However, current approaches must make trade-offs between signal quality and longevity which limit their clinical potential. To address this issue, we have developed the regenerative peripheral nerve interface (RPNI) and tested its use in non-human primates. *Approach*. The RPNI consists of a small, autologous partial muscle graft reinnervated by a transected peripheral nerve branch. After reinnervation, the graft acts as a bioamplifier for descending motor commands in the nerve, enabling long-term recording of high signal-to-noise ratio (SNR), functionally-specific electromyographic (EMG) signals. We implanted nine RPNIs on separate branches of the median and radial nerves in two rhesus macaques who were trained to perform cued finger movements. *Main results.* No adverse events were noted in either monkey, and we recorded normal EMG with high SNR (>8) from the RPNIs for up to 20 months post-implantation. Using RPNI signals recorded during the behavioral task, we were able to classify each monkey's finger movements as flexion, extension, or rest with >96% accuracy. RPNI signals also enabled functional prosthetic control, allowing the monkeys to perform the same behavioral task equally well with either physical finger movements or RPNI-based movement classifications. *Significance*. The RPNI signal strength, stability, and longevity demonstrated here represents a promising method for controlling advanced prosthetic limbs and fully restoring natural movement.

S Online supplementary data available from stacks.iop.org/JNE/13/046007/mmedia

Keywords: peripheral nerve, prosthesis control, chronic recording

(Some figures may appear in colour only in the online journal)

## Introduction

Loss of even part of the upper limb is a devastating injury, and current available prostheses cannot fully restore natural function. An estimated 20%–40% of upper-limb amputees reject using a prosthesis [1, 2], mostly citing the lack of functionality [3, 4]. Fully-articulated myoelectric prostheses, which use voluntary activation of residual muscles as a control signal, promise the restoration of multiple naturally-controlled degrees of freedom. However, the rejection rate for

[6] Author to whom any correspondence should be addressed.

 

this state-of-the-art technology is not significantly better than that of simple body-powered hooks [1, 5].

The primary underlying issue with this technology is the scarcity of independent signals with which to control all of the available functions of the prosthesis. Direct prosthetic control, in which each recorded muscle is mapped to its corresponding physiological function on the prosthesis [6], would reduce the user's cognitive burden while operating the prosthesis and allow for intuitive, simultaneous control of multiple degrees of freedom. However, this requires a separate, independent control signal for each degree of freedom, which is not possible for standard surface electromyography (EMG) on an amputee due to a combination of inadequate remaining musculature, signal cross-talk contamination, and attenuation of deep muscle signals at the skin surface. This leads to either a reduced set of functions available to the user or non-physiological control strategies which require long and tedious training periods, both of which may contribute to rejection of the prosthesis.

An ideal solution to this problem is to record motor commands directly from peripheral nerves, which are still extant in the residual limb and carry information about the amputated musculature. However, this is difficult to accomplish in practice. Signals recorded by epineural electrodes are typically low amplitude and corrupted by much larger EMG activity from the surrounding muscles [7, 8]. More selective and higher amplitude signals can be recorded by penetrating intraneural electrodes [9], but damage to the nerve may result in shortened implant lifetime.

Targeted muscle reinnervation (TMR) solves many of the issues with both myoelectric and direct nerve interfaces, and has been successfully demonstrated in several amputees [10, 11]. A hybrid approach, the TMR procedure reroutes transected nerves from the arm into sections of denervated muscles in the chest or residual limb. After the muscles are reinnervated by the rerouted nerves, they produce large amplitude EMG activity in response to voluntary motor commands. These biologically amplified signals are recorded by high-density surface electrodes, and serve to increase the number of available physiologically-relevant control sites. Through TMR, patients have been able to use advanced multi-functional robotic limbs, controlling elbow and wrist movement along with up to four hand grasps with no mode selection required [10].

The primary limitation of TMR, however, is that because whole nerves are attached to large sections of muscle, separate functional signals are not well isolated [12] and nerve fibers controlling any particular function are not guaranteed to reinnervate the new muscle [13]. This limits the number of independent control signals enabled by TMR. To overcome this, recent efforts have focused on pattern recognition algorithms to classify intended movement from a large number of electrodes covering the entire reinnervated area [10, 14]. Though the user can select and initiate a large number of movements with this control scheme, they are largely limited to sequential movements in which one degree of freedom is activated at a time, increasing both the controller complexity and the required user training time. Additionally, the need to cover a large area may prohibit the use of implanted intramuscular electrodes, which would produce a much more stationary signal. This non-stationary signal in turn requires either frequent re-training of the controller or careful maintenance of the electrode interface, such as regularly taking off the prosthesis to dry accumulated sweat before continuing use [12].

To address these issues, we have developed the regenerative peripheral nerve interface (RPNI), which consists of a small, autologous partial muscle graft which has been reinnervated by a transected peripheral nerve branch. Following initial implantation, the muscle graft temporarily degenerates due to lack of innervation and vascularization. During this time, cells in the graft periphery are sustained via diffusion from the surrounding tissue [15]. Over the course of several months, the graft is revascularized, regenerates (creating new, healthy muscle fibers), and is reinnervated by the transplanted nerve through axonal sprouting and elongation within the graft [16, 17]. The mature, reinnervated RPNI then produces high-amplitude EMG activity in response to voluntary motor commands [18]. The muscle graft thus acts as both a stable housing for the nerve and a biological amplifier for descending action potentials in the nerve.

Like TMR, the RPNI creates new physiologic EMG recording sites for natural control of multiple degrees of freedom. However, using small muscle grafts instead of large intact muscles enables several advantages. First, RPNIs can be placed directly at the distal end of the nerve without rerouting the nerve into the large muscles of the chest or residual limb. This allows for the use of RPNIs with any level of amputation, and requires a less invasive surgical procedure. Second, RPNIs can be made more functionally selective by intraneural dissection of the residual nerve into fascicles and implanting separate RPNIs on each of these fascicles. By pairing each RPNI with an intramuscular EMG electrode, we can potentially record stable, independent signals from each fascicle in the nerve and implement more natural and effective prosthetic control schemes.

The long-term viability of RPNIs has been previously reported in a rat model [19], demonstrating that RPNIs are successfully reinnervated and maintain health and electrical responsiveness up to 7 months post-implantation. A further study found that implanted RPNIs produced high-amplitude, physiologically-appropriate EMG activity in response to volitional movement during walking in rats [18]. In order to test the safety and performance of this technique in the context of voluntary finger movements, we implanted RPNIs in the forearms of two healthy rhesus macaques. We recorded volitional EMG signals from the RPNIs during a finger movement task, and conducted a preliminary assessment of both the signal quality and the ability to extract functional information from the recorded signals in order to control a prosthetic hand.

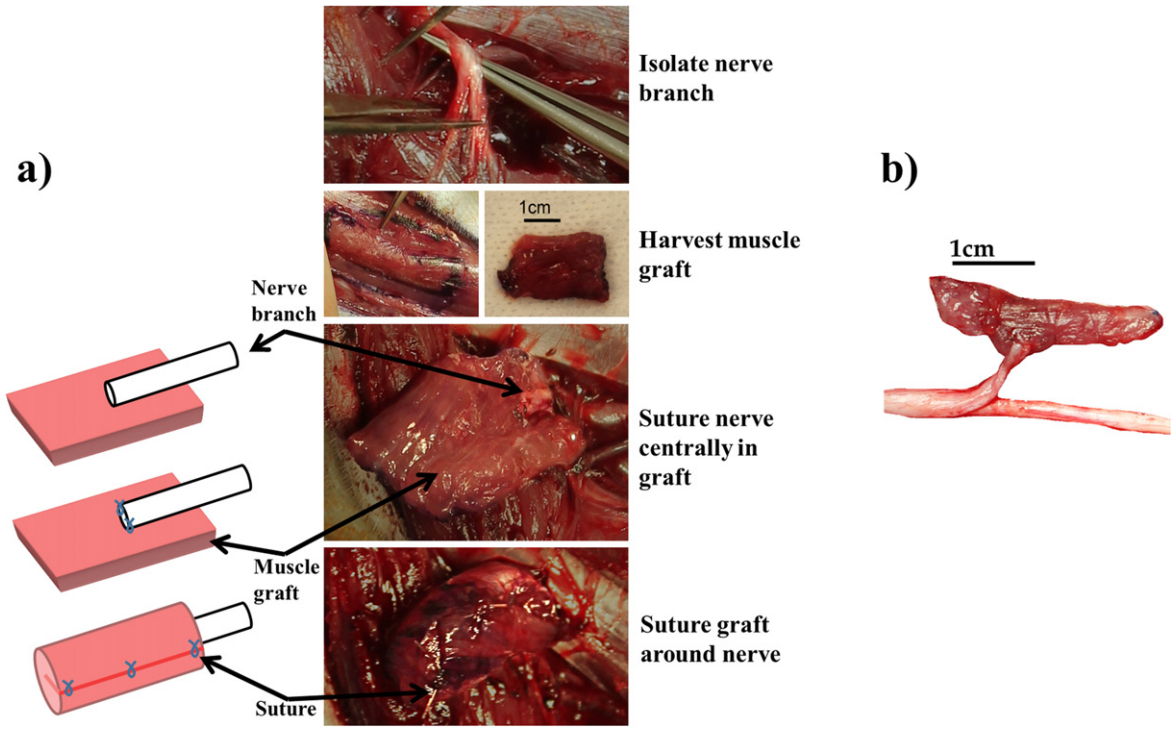


**Figure 1.** (a) RPNI implantation procedure illustrated from *top* to *bottom*. (b) A newly implanted RPNI, with a branch of the median nerve sutured into the muscle belly.

## Methods

All procedures were approved by the University of Michigan University Committee on the use and care of animals.

### *RPNI construction and implantation*

The process of RPNI construction is demonstrated in figure 1(a). First, the distal end of the target peripheral nerve is identified, isolated, and, if necessary, dissected into smaller branches or individual fascicles. For each resulting nerve, a small muscle graft, approximately $1 \times 3$ cm, is harvested from any healthy, native donor muscle. The distal end of each nerve is then placed centrally in its corresponding muscle graft and secured in place with sutures from epineurium to epimysium. The muscle graft is then folded around the nerve to create a stable housing and sutured together. A newly-constructed RPNI is shown in figure 1(b).

Implantation of multiple RPNIs is achieved by making small access incisions over the nerves of interest and the muscle for harvesting grafts. The above procedure is then simply repeated as necessary to create the desired number of RPNIs. Once implanted, RPNIs can be placed anywhere in the limb, but in most cases would be left at the original site of the nerve ending in order to minimize anatomical disruption.

Following these procedures, we implanted a total of nine RPNIs on separate branches of the median and radial nerves in the forearms of two rhesus macaques L and R. These branches terminated on the extrinsic finger flexors and extensors, providing a basis for prosthetic hand control. To preserve motor function, we transected only minor, redundant terminal motor nerve branches (see table 1 in the Results for details of each RPNI).

### *Electrophysiology*

During the first RPNI implantation surgery, we implanted several bipolar epimysial EMG electrodes (Plastics One). The electrodes consisted of insulated stainless steel leads attached to a silicone backing. The electrodes were placed on the surface of the RPNI muscle grafts and secured in place by wrapping small intestinal submucosa (SIS) around the muscle-electrode construct and suturing it together. The leads were then tunneled subcutaneously along the arm and back to a connector on the animal's headcap. Leads were looped at the RPNIs and at each joint for strain relief.

Shortly after surgery, the animal was able to break the leads at the margin of the headcap, leaving no intact electrodes for recording. In a revision surgery, it was noted that the stiffness of the silicone patch had caused significant scar formation and presumably impeded RPNI regeneration, so the epimysial electrodes were extracted and not used further on either animal.

Prior to chronic electrode implantation in both animals (during epimysial electrode extraction in the first animal and during the initial implantation surgery in the second animal), RPNIs were placed superficially in the subcutaneous plane in order to facilitate acute, percutaneous recording. During task behavior, we recorded EMG from the superficial RPNIs via fine-wire electrodes (Natus Medical). The RPNIs were located using surface landmarks and surgical photos. The wires were inserted into the RPNI muscle via hypodermic needle.

**Table 1.** Details of implanted RPNIs.

| Monkey | RPNI name | Nerve | Nerve branch function | Donor muscle |
|---|---|---|---|---|
| L | FDSa | Median | Flexion of digits 2–5 (PIP, MCP joints) | FCR |
| | FDSb | Median | Flexion of digits 2–5 (PIP, MCP joints) | FDS |
| | FDPa | Median | Flexion of digits 1–3[a] (DIP, PIP, MCP joints) | FCR |
| | FDPb | Median | Flexion of digits 1–3[a] (DIP, PIP, MCP joints) | FCR |
| | EDCa | Radial | Extension of digits 2–5 (DIP, PIP, MCP joints) | EDC |
| R | FDSc | Median | Flexion of digits 2–5 (PIP, MCP joints) | FCR |
| | FDPc | Median | Flexion of digits 1–3[a] (DIP, PIP, MCP joints) | FCR |
| | FDPd | Median | Flexion of digits 1–3[a] (DIP, PIP, MCP joints) | FCR |
| | EDCb | Radial | Extension of digits 2–5 (DIP, PIP, MCP joints) | EDC |

[a] In the macaque, *flexor pollicis longus* does not exist and FDP includes a tendon to the thumb [22].
FDS—flexor digitorum superficialis, FDP—flexor digitorum profundus, EDC—extensor digitorum communis, FCR—flexor carpi radialis, DIP—distal interphalangeal joint, PIP—proximal interphalangeal joint, MCP—metacarpophalangeal joint.

As the RPNIs were located directly subcutaneously, the needle was inserted at a shallow angle and advanced just far enough to bury both contacts under the skin in order to avoid contact with the muscle within the deep compartments. Recording locations were verified in further revision surgeries. Percutaneous recordings of healthy, intact muscles were also obtained for comparison.

To subsequently facilitate chronic recording of RPNI activity, we implanted bipolar intramuscular electrodes (IM-MES, Ardiem Medical). The IM-MES electrodes consist of two insulated stainless steel leads coiled in a double helix formation and potted in silicone tubing [20]. Contacts are formed by exposing the leads and wrapping them around the tubing, and a polypropylene anchor at the distal end secures the electrode in the muscle. In the first animal, the two contacts on the electrode were 4 mm long with a diameter of 1.27 mm (the diameter of the silicone tubing), and were separated by 6 mm. After noting that, in some cases, this was too large to fit both contacts within the muscle belly of an RPNI, a reduced contact size of 1.5 mm and inter-contact spacing of 2.5 mm were used for the second animal. A single IM-MES electrode was placed in the muscle belly of each RPNI, as well as in a healthy control muscle, by making a small incision and manually feeding the electrode anchor-first into the muscle. Leads were tunneled subcutaneously to a transcutaneous port on the animal's back and attached to a connector protected by a primate jacket.

During task performance, EMG signals from the RPNIs were input into either a DAM50 differential EMG amplifier (WPI), which filtered the signal between 10 and 1000 Hz with a gain of 1000x, or directly into a Cerebus neural signal processor (Blackrock Microsystems), which filtered the signal between 3 and 7000 Hz (unity gain). For real-time signal analysis, the Cerebus was used to record from multiple electrodes simultaneously. The DAM50 was used for lower-noise recordings of a single electrode. In both cases, the processed signal was digitized and saved to disk by the Cerebus at 30 ks $s^{-1}$. The signal was further sent from the Cerebus to the behavioral rig via ethernet, where it could be processed in real-time.

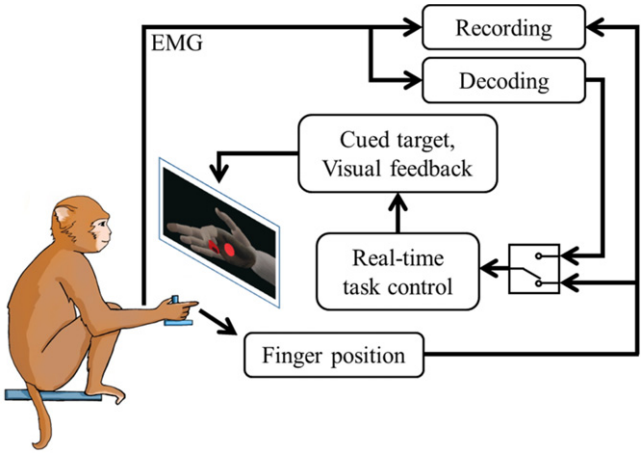


**Figure 2.** Monkey behavioral task. The monkey was required to hit virtual targets by moving his four fingers simultaneously. The virtual hand could be controlled either by the monkey's movements directly (as measured by flex sensors) or by EMG signals decoded into movement predictions in real-time, allowing either open-loop or closed-loop task performance.

During several revision surgeries after RPNI maturation in both animals, we tested the mature RPNIs for reinnervation and tissue health by evoking compound muscle action potentials (CMAPs) via stimulation of the implanted nerve. Using a Teca Synergy evoked potential system (Viasys Healthcare), we either stimulated the nerve just proximal to the point of entry to the RPNI or stimulated the muscle of the RPNI itself while simultaneously recording from bipolar electrodes in the belly of the RPNI muscle. Stimulation parameters varied between surgeries, consisting primarily of a pulse width of 200 $\mu$s and current amplitude between 1 and 20 mA when stimulating the nerve directly and a pulse width of 20 or 200 $\mu$s and current amplitude between 30 and 60 mA when stimulating the nerve through the RPNI muscle.

### *Behavioral task*

We trained both monkeys to perform a finger movement task, illustrated in figure 2. A flex sensor (Spectra Symbol) was

attached to the monkey's index finger, which fed finger position data to a real-time computer running xPC Target (Mathworks). A virtual model of a monkey hand was displayed in front of the monkey on a monitor, and mirrored the finger movements measured by the flex sensor. The monkeys both performed movements with all four fingers simultaneously, with the position of all four indicated by the index flex sensor. At the start of a trial, the xPC cued a spherical target to appear in the path of the virtual finger. The monkey was then required to move his fingers in order to hit the target on the screen. After holding the virtual finger in the target for a required hold time (usually set to 500–700 ms), the monkey was given a juice reward. The virtual hand could also be controlled by decoding the RPNI signals in real-time into predicted movement. The monkey would receive a reward only if the predicted movement was correct, and could act to correct the decode within the trial time limit in a closed-loop manner.

### *Signal analysis and decoding*

To isolate the EMG signal from motion and electrical artifacts, we filtered the data between 100 and 500 Hz using a second-order Butterworth filter. In offline analysis, the data were filtered forwards and backwards in order to eliminate phase shift.

For each recorded RPNI and intact muscle, we calculated both the maximum voluntary contraction (MVC) and the signal to noise ratio (SNR). MVC was calculated by isolating periods of maximum agonist behavior, corresponding to either full finger flexion or full finger extension movements, depending on the function of the RPNI nerve. Movement periods were isolated and labeled by thresholding the finger position and velocity to ensure both maximum EMG activation and consistent behavior. The mean of the peak-to-peak amplitude during all such movements was taken as the MVC. SNR was calculated by simply dividing the MVC by the noise floor for that channel, which was extracted by manually selecting quiescent periods in the signal and calculating the mean peak-to-peak amplitude.

In order to directly assess the functional efficacy of the RPNI signals, we classified current finger movement state using a Naïve Bayes classifier. Linear discriminant analysis was also performed, but classification accuracy was similar to that of the Naïve Bayes. As the decoding features, we extracted four temporal characteristics of the EMG waveform [14, 21] in successive 50 ms time bins: (1) mean absolute value, (2) number of zero crossings, (3) number of slope changes, and (4) waveform line length. These features were extracted simultaneously from one flexor RPNI and one extensor RPNI in each monkey, allowing classification of both flexion and extension. This was performed both offline and online in closed-loop. During closed-loop decoding, three targets were presented to the monkey, requiring flexion, extension, and no movement (i.e. maintaining a neutral, relaxed hand position), respectively. After training the classifier on the first ~200 trials of normal task performance, the virtual hand was switched to mirror the classifier output instead of the monkey's actual finger position. To smooth the prediction, the final classifier output was updated only after four consecutive identical predictions. The virtual finger was automatically positioned in the target space associated with the current prediction, and the monkey was required to make the classifier output the correct state for the entire hold time (at least ten consecutive time bins) in order to complete the task.

## Results

A total of nine RPNIs were implanted on separate branches of the median and radial nerves in the forearms of two rhesus macaques, L and R. Pictures of several of the implanted RPNIs for each monkey are shown in figure 3, and the anatomical details of each RPNI are shown in table 1. RPNI names are based on the muscle originally innervated by the transected nerve branch, with a letter differentiating RPNIs with the same function. Branches of the median and radial nerves were chosen in order to represent functions which would be active during the behavioral task. As any healthy muscle tissue can be used for grafting, muscles nearby each nerve branch were chosen as donors in order to minimize the number of required incisions.

A timeline of surgical procedures and electrophysiology recordings is shown in figure 4. In particular, note in Monkey L that EMG was recorded from the RPNIs up to 20 months post-implantation, and RPNIs were subsequently deemed healthy at the time of removal. Recordings were taken from Monkey R up to 14 months post-implantation, until experiments were completed. Monkey R's RPNIs and IM-MES electrodes have not been removed in order to facilitate long-term investigation of electrode implantation effects.

### *RPNIs caused no health issues*

No major health concerns were noted by laboratory or veterinary staff during a 10 d post-op monitoring period or afterwards. In order to minimally disrupt normal function of the limb, we transected only small terminal nerve branches (leaving intact several other branches of the median and radial nerves innervating the FDS, FDP, and EDC muscles in the arm), and harvested only small (approximately $1 \times 3$ cm) grafts from large native FCR, FDS, and EDC muscles for each RPNI. Generally, muscle grafts can be harvested from any location, but here were taken from the implanted arm to limit the number of surgical sites. Following veterinary recommendation, buprenorphine was administered during the first 24 h following each surgery, and carprofen and cefazolin administered for the first week to control possible pain and prevent wound infection. Both monkeys had minor swelling of the limb and hand immediately after one surgery (the second of three surgeries in Monkey L and the first of two in Monkey R), but this was attributed to the compression bandage applied at the end of surgery and not to the RPNI procedure itself. Both monkeys regained full use of the hand and limb within three days post-surgery, except in the case of

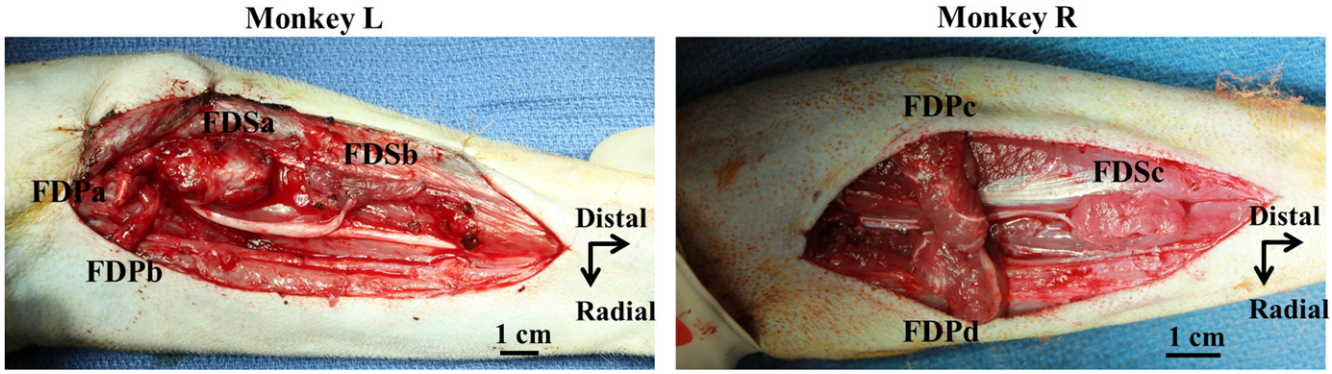


**Figure 3.** RPNIs implanted in the forearm of two monkeys (left—Monkey L, right—Monkey R), labeled as listed in table 1. All RPNIs in Monkey R and the FDSb RPNI in Monkey L are newly implanted, while the other RPNIs in Monkey L are mature and reinnervated.

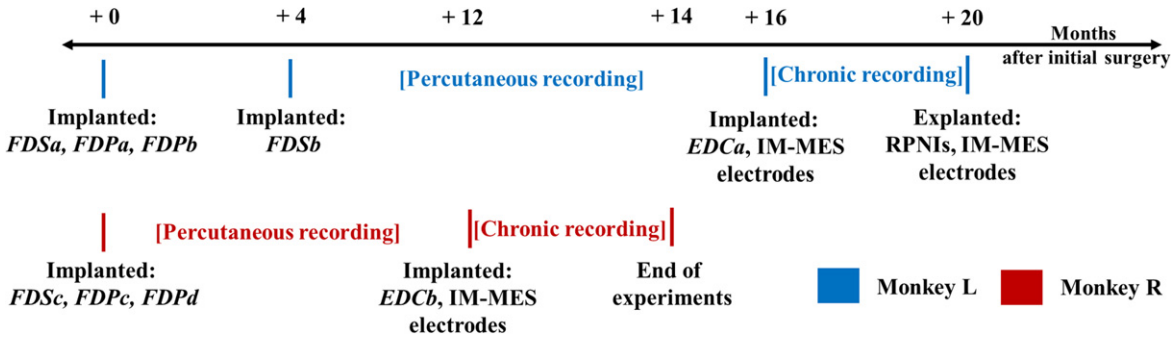


**Figure 4.** Timeline of RPNI surgeries, including both RPNI creation and chronic electrode implantation, and electrophysiology experiments. EMG was recorded from RPNIs in Monkey L up to 20 months post-implantation and from RPNIs in Monkey R up to 14 months post-implantation.

Monkey R's swelling in which the animal recovered full use after one week, following fluid drainage by veterinary staff.

### *RPNIs successfully reinnervated and regenerated*

All RPNIs appeared to regenerate and reinnervate successfully, producing healthy muscle tissue and an active neural connection. Visual inspection of RPNIs during revision surgeries indicated vascularized muscle grafts and integrated nerves. Because the EDCa RPNI in Monkey L was co-implanted with a chronic electrode upon initial implantation, it provided a clear illustration of the regeneration process. The EDCa RPNI is shown in figure 5(a), at the time of implantation and at the time of graft explantation four months later. As is typical, the mature muscle graft is somewhat smaller than the original graft, but is well vascularized and appears healthy. Darkened areas on the muscle are due to ink staining from a marker used during surgery to outline the tissue to be harvested (in the top implantation picture), and to a small amount of bleeding during RPNI extraction (in the bottom explantation picture). Histological staining (hematoxylin and eosin) of this RPNI, shown in figure 5(b), revealed healthy tissue with no evidence of necrosis. The RPNI muscle fibers are somewhat smaller than in intact tissue, but the increased proportion of centrally-located nuclei and the more rounded shape of the RPNI fibers may also indicate that regeneration was still ongoing [23]. During the explantation surgery (at four months post-implantation, prior to tissue extraction), stimulation of the EDCa nerve produced CMAPs in the RPNI, indicating a healthy neuromuscular interface, as shown in figure 5(d). Additionally, as a chronic intramuscular electrode was placed in the EDCa RPNI at implantation, we were able to track the degree of innervation over time, measured by the amplitude of the recorded signal during task performance. This is shown in figure 5(c) as the signal amplitude during MVCs, compared to the equivalent signals recorded from an intact wrist muscle and a previously-matured RPNI. Note that only the EDCa RPNI shows an increasing trend in the signal amplitude, indicating reinnervation over a period of ~3 months, while the mature FDPb RPNI and intact ECR (*extensor carpi radialis)* remain stable.

No RPNIs failed to reinnervate, however it appeared that some RPNIs, particularly in Monkey R, reintegrated somewhat with the surrounding tissue. This made it more difficult to isolate the RPNI to place electrodes, and likely increased the amount of cross-talk picked up from nearby musculature. This may have been due to the non-use of SIS for these RPNIs, a smaller nerve transplant, or the swelling after Monkey R's initial implantation surgery. Even in these cases, however, the nerve was still intact and RPNI remain innervated as verified by intra-operative stimulation and visualization of healthy tissue.

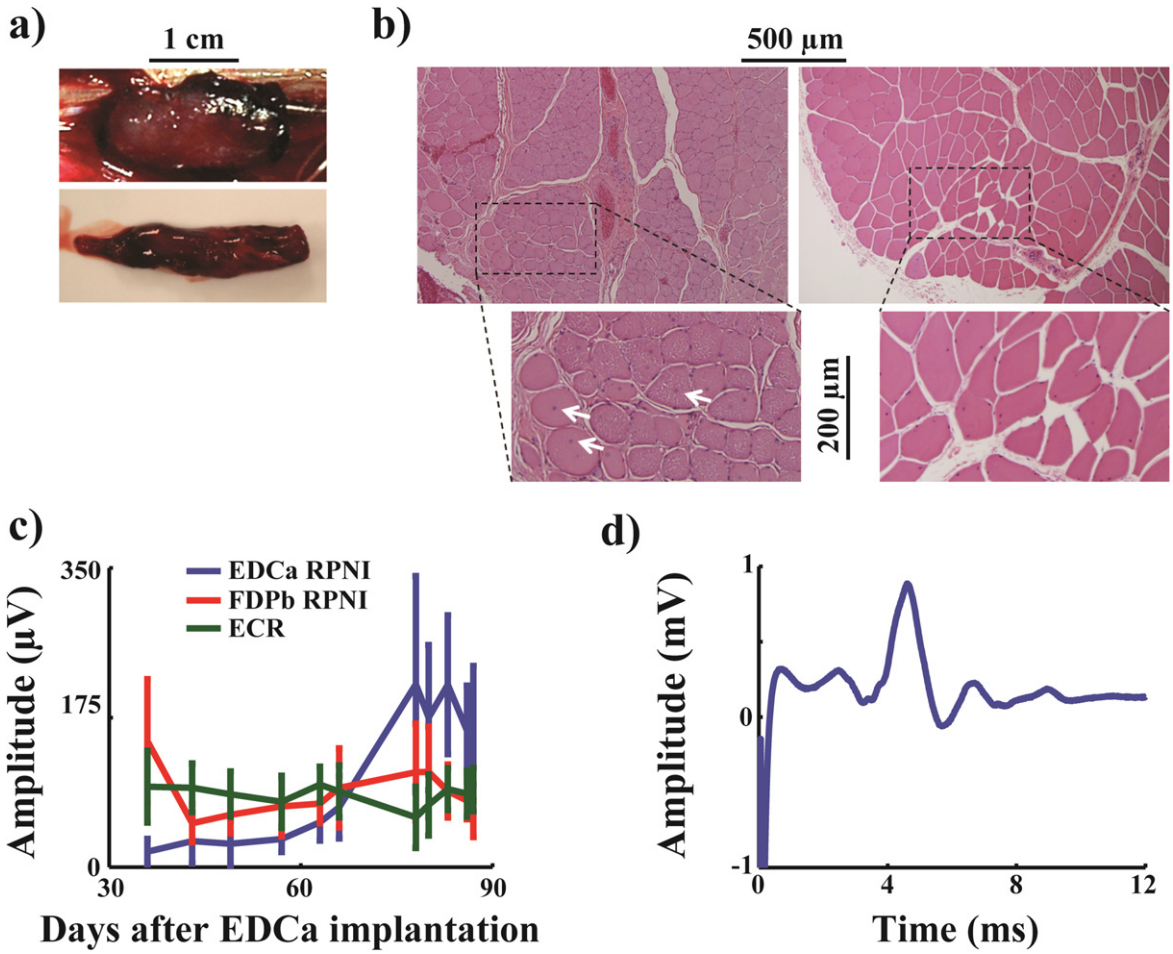


**Figure 5.** (a) EDCa RPNI at implantation (*top*) and after 3 months of maturation (*bottom*). (b) EDCa RPNI histology (H&E staining) after maturation (*left*) and comparison to intact FDS muscle (*right*). White arrows highlight some of the fibers presumably undergoing regeneration. (c) Signal amplitude over time for the recently-implanted EDCa RPNI (*blue*), the matured FDPb RPNI (*red*), and the intact ECR muscle (*green*). (d) Mean CMAP produced by the EDCa RPNI in response to intra-operative stimulation.

### *RPNIs produce normal, volitional EMG*

Signals recorded from RPNIs via both acute and chronically-implanted electrodes appeared similar to intact control muscles. EMG was correlated with the expected physical behavior of each nerve branch (either flexion or extension of the fingers), and single motor units could be discriminated from all RPNIs. Example IM-MES recordings are shown for several RPNIs and intact muscles in figure 6, along with single unit action potentials extracted from each. In the bottom right trace of figure 6, the intact EDC signal was recorded from the IM-MES electrode originally placed in the EDCb RPNI. However, as the signal amplitude was very high immediately after implantation (which could not be produced by a denervated muscle), the electrode was assumed to have slipped out of the RPNI and was recording from the surrounding EDC muscle. It is included here as a healthy control muscle for comparison. Correct electrode locations in Monkey L were visually confirmed during RPNI explantation.

Though RPNI signal amplitudes varied, and were generally smaller in Monkey R, SNRs were high. This indicates that even with smaller amplitude signals, selective information can still be easily extracted from the RPNIs.

Cross-talk injected from nearby intact muscles was seen on several RPNIs, most likely due to incomplete implantation of the electrode in the RPNI (in several RPNIs, the proximal contact on the lead was located at least partially outside the muscle graft). In the left column of figure 6, the EDCa RPNI signal is correlated with finger extension (as expected) and at least somewhat with finger flexion, probably corrupted by the nearby wrist extensor ECR (also shown in figure 6). This cross-talk was not seen in percutaneous fine-wire recordings, indicating that, as expected, a smaller electrode would reveal more local activity. Accordingly, the amplitude of the signals obtained from acute, percutaneous electrodes varied widely across sessions. Two example recordings are shown in figure 7. This variability could potentially be exploited in the future to obtain more information from each RPNI. It also indicates that higher amplitude signals could potentially be recorded by optimally placing smaller electrodes in the RPNI muscle belly, as the fine-wire recording of the FDPd RPNI in Monkey R in figure 7 displayed a higher amplitude than the IM-MES recording of the same RPNI shown in figure 6.

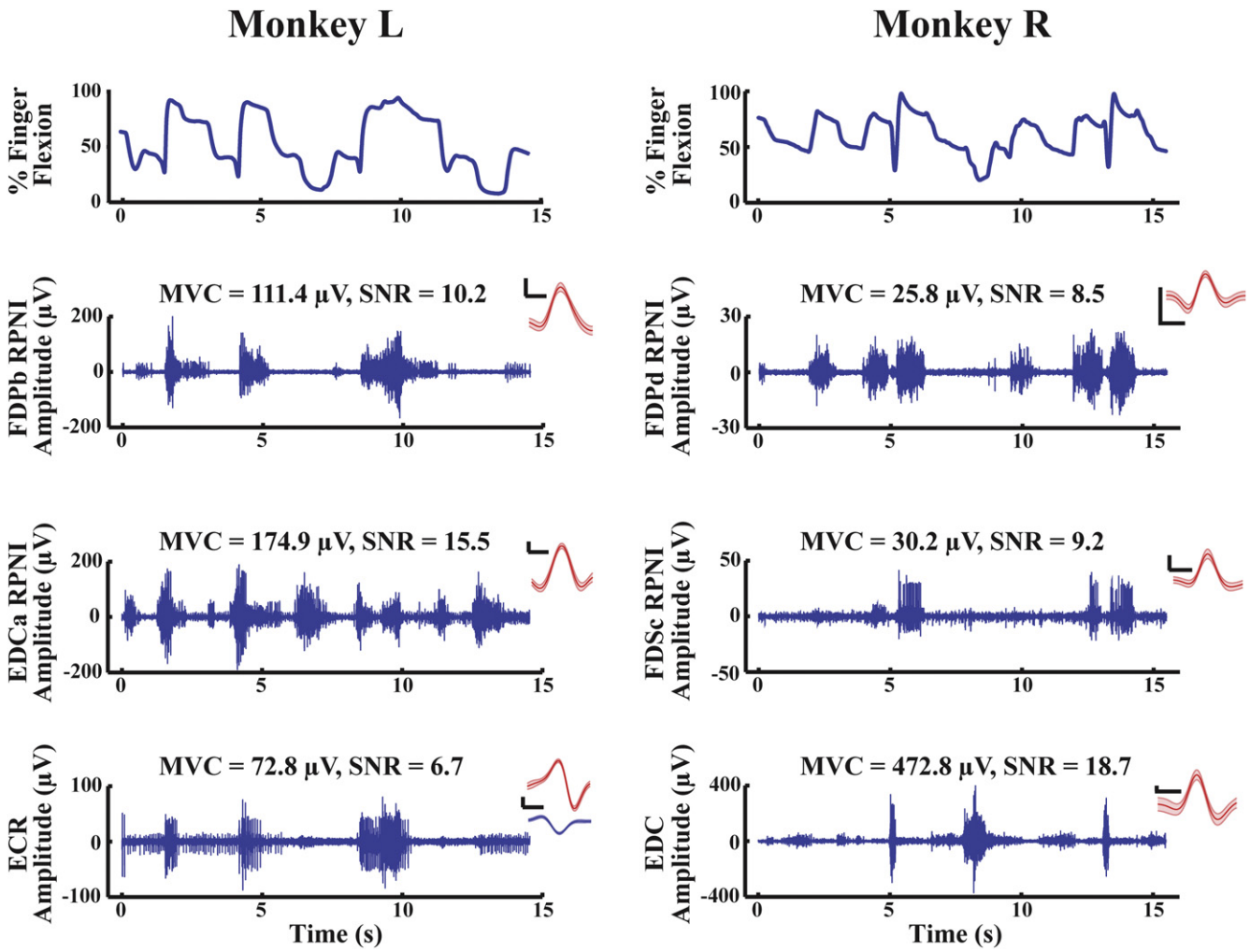


**Figure 6.** Example EMG recorded from chronic IM-MES electrodes in both monkeys (the *bottom* trace in each column is an intact muscle), with isolated single motor unit action potentials (to the *right* of each column—scale bars indicate 20 $\mu$V and 2 ms, respectively).

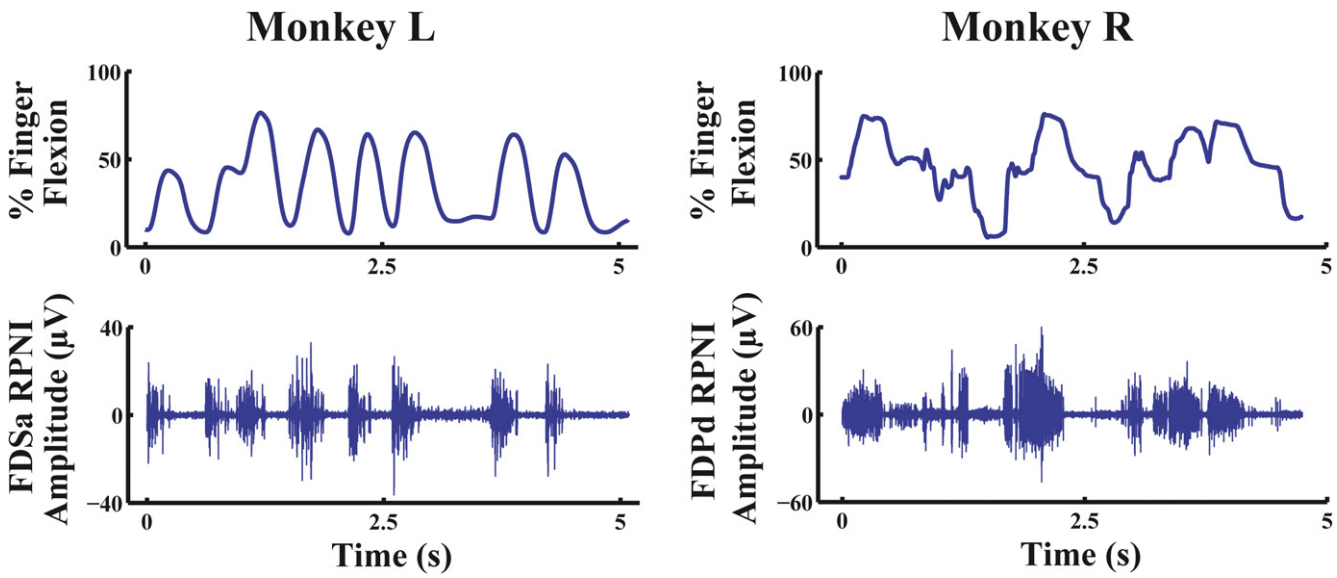


**Figure 7.** Example EMG recorded from acute fine-wire electrodes in both monkeys, showing signals which are qualitatively similar to those of the IM-MES recordings (although the fine-wire electrodes recorded higher amplitudes from the FDPd RPNI in Monkey R).

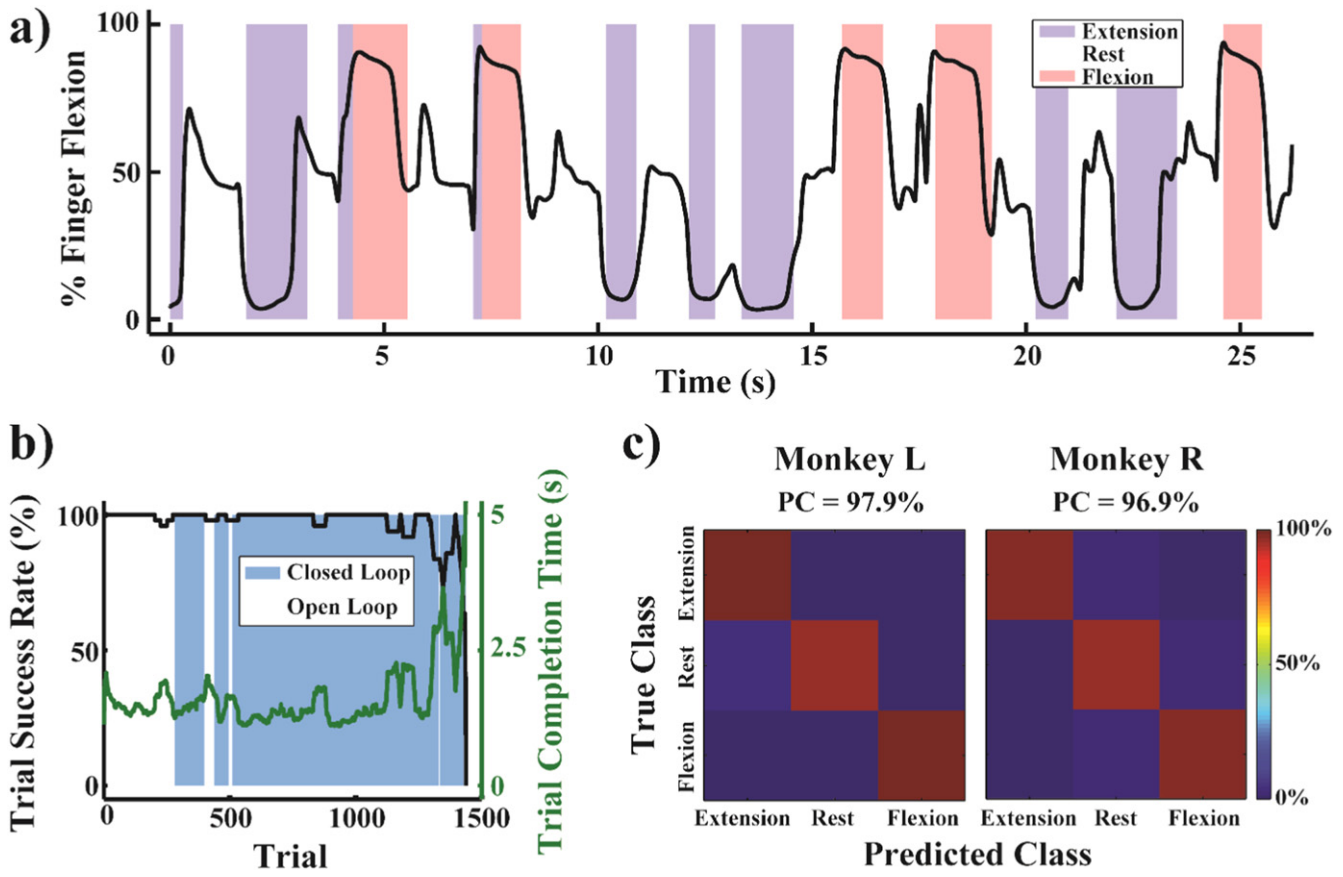


**Figure 8.** Classification of finger movement state using IM-MES electrodes: (a) online, open-loop during Monkey L task behavior—predicted movement state is overlaid as background on a trace of the monkey's actual finger movements. (b) Monkey L's task performance during physical control (*white background*) and closed-loop RPNI control (*blue background*). (c) For both monkeys, offline classification accuracy on the same day as the online experiment, using whole-trial data.

### *RPNIs can provide functional prosthesis control signals*

Using a simple Naïve Bayes classifier, we were able to decode RPNI signals both offline and in real-time to allow the monkeys to control a virtual hand. In offline decodes of 280 and 447 successful finger movement trials for Monkey L and Monkey R, shown in figure 8(c), we classified hand posture as either extension, flexion, or rest with an accuracy of 97.9% correct and 96.9% correct, respectively. We used leave-one-out cross-validation to minimize overfitting, and computed signal features using the whole trial (~1.5 s of activity, depending on the directness of the monkey's movement to the target) to ensure the inclusion of the maximum amplitude EMG bursts during movement. Because we used the whole trial for classification, true posture labels were based on the target position for that trial, whether or not the monkey moved monotonically towards the target.

Online classification was performed with both monkeys using 50 ms bins. To remove jitter on the output, we required four identical, consecutive decodes before changing the final classification. An example online decode is shown in figure 8(a) for Monkey L. The classifier accurately transitions between movement states, depending on the monkey's current hand posture. Notably, the decode is relatively robust to noisy behavior, correctly classifying rest posture even when the monkey over- or under-shoots the neutral target (i.e. 50% flexion). This indicates that a deliberate attempt at movement was required for correct classification, minimizing the amount of false-positive detections, which may be a desirable trait in a final myoelectric controller. See supplemental video 1 for a video of online, open-loop decoding actuating an i-limb ultra prosthetic hand (Touch Bionics), during a separate experimental session using a single percutaneous electrode in the FDSa RPNI of Monkey L.

To quantify the ability of this classification to provide useful prosthetic control, we allowed the monkey to perform the behavioral task in both physical control (in which the virtual hand is controlled by the monkey's actual movements) and closed-loop RPNI control (in which the virtual hand is controlled by the online classifier output). Monkey L's success rate and trial completion time (averaged over a 50-trial window) are shown in figure 8(b), during physical and RPNI control. The required hold time for a successful target acquisition was 700 ms (equivalently, at least 14 consecutive correct classifications). Because the trial timeout (after which the trial was declared unsuccessful) was a relatively long 10 s, the monkey's success rate was generally near 100%. However, the average trial completion time during physical control was 1.5 s and was 1.4 s during RPNI control, indicating that the monkey was able to perform the task equally well with

either controller. Note also that there is no obvious adjustment period when first switching to RPNI control, demonstrating the natural, physiologic control provided by the RPNIs. See supplemental video 2 for a video of closed-loop task performance in Monkey L.

## Discussion

We have provided compelling initial safety data for the RPNI technique in two non-human primates, demonstrating that the implantation of nine RPNIs caused no health concerns and did not noticeably affect the normal function of un-modified anatomy. Further, we have shown that this approach produces healthy tissue which generates normal EMG signals with a high SNR. These signals could be easily recorded using acute or chronically-implanted electrodes and decoded into functional prosthesis commands, showing promise as a capable, intuitive control source. The behavioral task and decodes presented here are a single degree of freedom, making it substantially equivalent to commercial products which provide 'open' and 'close' signals.

Though promising, further investigation is required to answer some remaining questions. Primarily, the number of independent signals produced by the RPNIs could not be verified due to the requirements of monkey behavioral training. Thus it remains to be seen whether fully independent signals can be obtained from each RPNI, and whether this would enable the simultaneous control of multiple degrees-of-freedom. This issue may be complicated at more proximal levels of amputation by the greater number of functions represented in each nerve, though this can potentially be mitigated by dissection of the nerve into discrete fascicles. Further, here the RPNIs were implanted in able-bodied monkeys and great care was taken to minimize any resulting motor deficits, limiting the placement of RPNIs onto small terminal nerve branches which were surrounded by intact muscles performing similar physiological functions. This made it difficult to quantify any potential cross-talk from neighboring muscles. We expect that this effect was minimal, due to the inherent selectivity of intramuscular electrodes, the verification of healthy regenerated RPNI tissue, and previous work in rats [18]. However, this must be confirmed in future human studies by recording activity that could not be generated by residual anatomy.

Despite these limitations, this is the first demonstration of prosthesis control via an interface capable of providing stable, long-term physiological control at any level of amputation. Decoding of finger movements and subsequent closed-loop control of prosthetic devices (or the virtual equivalent) has been previously demonstrated using both surface [24] and intramuscular [25–27] EMG. Though these interfaces have resulted in impressively high-performance control, the inherent instability of both surface and percutaneous fine-wire electrodes represents a significant challenge to their clinical implementation. Perhaps more importantly, however, providing intuitive prosthesis control via residual muscle EMG is not possible for amputees with more proximal injuries.

Direct nerve interfaces, which could be used for any level of injury, have also been used to provide prosthesis control but face their own set of challenges. The two electrode types which have been the most studied in terms of direct nerve recording and subsequent prosthesis control are the longitudinal intra-fascicular electrode [28] and the Utah electrode array [29]. Both have been implanted in multiple amputees and used to provide control functionality similar to this study [30, 31]. However, recorded signal amplitudes were generally small and corrupted by nearby EMG [9, 32]. Though these issues could be somewhat mitigated by further signal processing [9, 33] or physical shielding of the array [34], successful recording and control have not been demonstrated for longer than one month, with questions remaining as to nerve health under longer-term implantation of these electrodes.

Given these issues, the signal strength, stability, and longevity of the RPNI technique demonstrates promise as a clinically-viable technology. In future clinical practice, RPNI implantation could act as a supplement for residual musculature, creating new sites for myoelectric control to replace those lost during the amputation. Combining EMG recording of both residual muscle and RPNIs with a wireless implantable recording system, we can potentially restore full, effective control of a lost limb for the lifetime of the patient.

## Acknowledgments

This work was supported by the Wallace H Coulter Foundation, the Frederick A Coller Surgical Society, and the Plastic Surgery Foundation. P Vu, D Tat, and A Bullard were supported by NSF Graduate Research Fellowships.

## References

[1] Biddiss E A and Chau T T 2007 Upper limb prosthesis use and abandonment: a survey of the last 25 years *Prosthet. Orthot. Int.* **31** 236–57

[2] Raichle K A, Hanley M A, Molton I, Kadel N J, Campbell K, Phelps E, Ehde D and Smith D G 2008 Prosthesis use in persons with lower- and upper-limb amputation *J. Rehabil. Res. Dev.* **45** 961–72

[3] Biddiss E and Chau T 2007 Upper-limb prosthetics: critical factors in device abandonment *Am. J. Phys. Med. Rehabil.* **86** 977–87

[4] Wright T W, Hagen A D and Wood M B 1995 Prosthetic usage in major upper extremity amputations *J. Hand Surg.* **20** 619–22

[5] McFarland L V, Winkler S L H, Heinemann A W, Jones M and Esquenazi A 2010 Unilateral upper-limb loss: satisfaction and prosthetic-device use in veterans and servicemembers from Vietnam and OIF/OEF conflicts *J. Rehabil. Res. Dev.* **47** 299

[6] Roche A D, Rehbaum H, Farina D and Aszmann O C 2014 Prosthetic myoelectric control strategies: a clinical perspective *Curr. Surg. Rep.* **2** 1–11

[7] Navarro X, Krueger T B, Lago N, Micera S, Stieglitz T and Dario P 2005 A critical review of interfaces with the peripheral nervous system for the control of neuroprostheses

and hybrid bionic systems *J. Peripher. Nervous Syst.* **10** 229–58

[8] Sahin M, Haxhiu M A, Durand D M and Dreshaj I A 1997 Spiral nerve cuff electrode for recordings of respiratory output *J. Appl. Physiol.* **83** 317–22

[9] Clark G A, Wendelken S, Page D M, Davis T, Wark H A C, Normann R A, Warren D J and Hutchinson D T 2014 Using multiple high-count electrode arrays in human median and ulnar nerves to restore sensorimotor function after previous transradial amputation of the hand *36th Annual Int. Conf. of the IEEE Engineering in Medicine and Biology Society (EMBC) 2014* pp 1977–80

[10] Kuiken T A, Li G, Lock B A, Lipschutz R D, Miller L A, Stubblefield K A and Englehart K 2009 Targeted muscle reinnervation for real-time myoelectric control of multifunction artificial arms *JAMA J. Am. Med. Assoc.* **301** 619–28

[11] Dumanian G A, Ko J H, O'Shaughnessy K D, Kim P S, Wilson C J and Kuiken T A 2009 Targeted reinnervation for transhumeral amputees: current surgical technique and update on results *Plast. Reconstructive Surg.* **124** 863–9

[12] Kuiken T A, Dumanian G A, Lipschutz R D, Miller L A and Stubblefield K A 2004 The use of targeted muscle reinnervation for improved myoelectric prosthesis control in a bilateral shoulder disarticulation amputee *Prosthet. Orthot. Int.* **28** 245–53

[13] Stubblefield K A, Miller L A, Lipschutz R D and Kuiken T A 2009 Occupational therapy protocol for amputees with targeted muscle reinnervation *J. Rehabil. Res. Dev.* **46** 481–8

[14] Zhou P, Lowery M M, Englehart K B, Huang H, Li G, Hargrove L, Dewald J P A and Kuiken T A 2007 Decoding a new neural machine interface for control of artificial limbs *J. Neurophysiol.* **98** 2974–82

[15] Faulkner J A, Maxwell L C, Mufti S A and Carlson B M 1976 Skeletal muscle fiber regeneration following heterotopic autotransplantation in cats *Life Sci.* **19** 289–96

[16] Cedars M G M D and Miller T A M D 1984 A review of free muscle grafting *Plast. Reconstructive Surg.* **74** 712–20

[17] Carlson B M and Faulkner J A 1983 The regeneration of skeletal muscle fibers following injury: a review *Med. Sci. Sports Exercise* **15** 187–98 [review]

[18] Ursu D C, Urbanchek M G, Nedic A, Cederna P S and Gillespie R B 2016 In vivo characterization of regenerative peripheral nerve interface function *J. Neural Eng.* **13** 026012

[19] Kung T A, Langhals N B, Martin D C, Johnson P J, Cederna P S and Urbanchek M G 2014 Regenerative peripheral nerve interface viability and signal transduction with an implanted electrode *Plast. Reconstructive Surg.* **133** 1380–94

[20] Memberg W D, Stage T G and Kirsch R F 2014 A fully implanted intramuscular bipolar myoelectric signal recording electrode *Neuromodulation Technol. Neural Interface* **17** 794–9

[21] Hudgins B, Parker P and Scott R N 1993 A new strategy for multifunction myoelectric control *IEEE Trans. Biomed. Eng.* **40** 82–94

[22] Serlin D M and Schieber M H 1993 Morphologic regions of the multitendoned extrinsic finger muscles in the monkey forearm *Cells Tissues Organs* **146** 255–66

[23] Cedars M G M D, Das S K M D, Roth J C B S and Miller T A M D 1983 The microscopic morphology of orthotopic free muscle grafts in rabbits *Plast. Reconstructive Surg.* **72** 179–87

[24] Tenore F V G, Ramos A, Fahmy A, Acharya S, Etienne-Cummings R and Thakor N V 2009 Decoding of individuated finger movements using surface electromyography *IEEE Trans. Biomed. Eng.* **56** 1427–34

[25] Cipriani C, Segil J L, Birdwell J A and Weir R F 2014 Dexterous control of a prosthetic hand using fine-wire intramuscular electrodes in targeted extrinsic muscles *IEEE Trans. Neural Syst. Rehabil. Eng.* **22** 828–36

[26] Birdwell J A, Hargrove L J, Weir R F F and Kuiken T A 2015 Extrinsic finger and thumb muscles command a virtual hand to allow individual finger and grasp control *IEEE Trans. Biomed. Eng.* **62** 218–26

[27] Smith L H, Kuiken T A and Hargrove L J 2014 Real-time simultaneous and proportional myoelectric control using intramuscular EMG *J. Neural Eng.* **11** 066013

[28] Lawrence S M, Dhillon G S, Jensen W, Yoshida K and Horch K W 2004 Acute peripheral nerve recording characteristics of polymer-based longitudinal intrafascicular electrodes *IEEE Trans. Neural Syst. Rehabil. Eng.* **12** 345–8

[29] Branner A and Normann R A 2000 A multielectrode array for intrafascicular recording and stimulation in sciatic nerve of cats *Brain Res. Bull.* **51** 293–306

[30] Rossini P M *et al* 2010 Double nerve intraneural interface implant on a human amputee for robotic hand control *Clin. Neurophysiol.* **121** 777–83

[31] Gasson M, Hutt B, Goodhew I, Kyberd P and Warwick K 2005 Invasive neural prosthesis for neural signal detection and nerve stimulation *Int. J. Adapt. Control Signal Process* **19** 365–75

[32] Dhillon G S, Lawrence S M, Hutchinson D T and Horch K W 2004 Residual function in peripheral nerve stumps of amputees: implications for neural control of artificial limbs1 *J. Hand Surg.* **29** 605–15

[33] Micera S *et al* 2011 Decoding of grasping information from neural signals recorded using peripheral intrafascicular interfaces *J. Neuroeng. Rehabil.* **8** 53

[34] Clark G A, Ledbetter N M, Warren D J and Harrison R R 2011 Recording sensory and motor information from peripheral nerves with utah slanted electrode arrays *Annual Int. Conf. of the IEEE Engineering in Medicine and Biology Society, EMBC 2011* pp 4641–4